

Time Series Photometry of the Dwarf Planet Eris

by

Rosemary E. Pike

Submitted to the Department of Earth, Atmospheric, and Planetary Sciences

in Partial Fulfillment of the Requirements for the Degree of

Bachelor of Science in Earth, Atmospheric, and Planetary Sciences

at the Massachusetts Institute of Technology

May 18, 2007 [June 2007]

Copyright 2007 Rosemary E. Pike. All rights reserved.

The author hereby grants to M.I.T. permission to reproduce and distribute publicly paper and electronic copies of this thesis and to grant others the right to do so.

Author _____

Signature redacted

Department of Earth, Atmospheric, and Planetary Sciences

May 18, 2007

Certified by _____

Signature redacted

Richard P. Binzel

Signature redacted Thesis Supervisor

Accepted by _____

Samuel Bowring

ARCHIVES



Chair, Committee on Undergraduate Program

The author hereby grants to MIT permission to reproduce and to distribute publicly paper and electronic copies of this thesis document in whole or in part in any medium now known or hereafter created.

Acknowledgements

Putting together a senior thesis has been quite a challenge—sometimes incredibly exciting and sometimes very frustrating. I would really like to thank everyone who helped me get through the frustrating parts and supported me in the exciting parts. In the end, I feel like I accomplished a great deal, thanks to my advisors, Dr. Henry Roe and Professor Richard Binzel, and the supportive environment of Course 12.

I began my project at Lowell Observatory during IAP of my senior year. Henry Roe provided a great dataset for me to work with and helped me through the analysis. He was never too busy to answer questions or help me with my IDL code. He was even willing to continue advising me over email during the spring semester. He was just incredibly supportive, even when I was incredibly far behind on my work, when my computer died, when I couldn't get the software... I never would have finished without his help.

At MIT, I was also advised by Rick Binzel. He helped me with all of the logistics of my thesis and was always positive and encouraging. He has been amazing about reading and commenting on my work and meeting with me all semester. My project turned out much better thanks to his input.

Finally, I would like to thank the rest of the Course 12 department, especially Professor James Elliot for moving my class project back so I could work on my thesis, and Jane Connor for providing writing support.

Table of Contents

Acknowledgements	2
Table of Contents	3
Figures and Tables	4
Abstract	5
Introduction	6
Eris or 2003UB313	6
Time Series Photometry	9
Anticipated Results	12
Previous Time Series Photometry of Eris	13
Data Collection	15
Methods	17
Analysis	26
Conclusions	28
Works Cited	29

Figures and Tables

Table 1	Properties of Eris	7
Figure 1	Eris and its Moon Dysnomia	8
Figure 2	EL61 Data from Rabinowitz et al. 2006	10
Figure 3	Swift Images of Eris	16
Figure 4	Image Comparison	16
Figure 5	Eris Magnitudes	18
Figure 6	Corrected Eris Magnitudes	20
Figure 7	Periodogram Results	21
Figure 8	Wrapped Plot of Eris Data	22
Figure 9	Magnitude Standard Deviations	23
Table 2	Detectable Signals	24
Figure 10	Comparison Data Plots	25

Time Series Photometry of the Dwarf Planet Eris

By Rosemary E. Pike

Submitted to the Department of Earth, Atmospheric, and Planetary Sciences

May 18, 2007

In Partial Fulfillment of the Requirements for the Degree of

Bachelor of Science in Earth, Atmospheric, and Planetary Sciences

Abstract

This project utilizes time series photometry to attempt to find the period of the newly discovered Kuiper Belt Object (KBO), Eris. Eris is known to have a radius slightly larger than Pluto and an extremely high albedo of 86%, indicative of fresh surface ices. This high albedo makes it likely that the brightness variations of Eris are small and difficult to detect. The data for this project were collected using the Swift Ultra Violet Optical Telescope (UVOT) over 29 nights. The 266 good images were analyzed using aperture photometry on Eris and 33 reference stars. A least squares fit was applied to correct for changes in overall image brightness, and Eris' magnitude was plotted over time. A periodogram was used to search for a periodic solution, but did not yield a significant signal. This means that the rotation period of Eris was below the detection limit of the data, so this detection limit was calculated. For a 6 hour period, the data would have had a 2 sigma significance for a full amplitude of 0.16 magnitudes, a 12 hour period is 0.125 magnitudes, an 18 hour period is 0.155 magnitudes, and a 24 hour period is 0.185 magnitudes. Knowing the detection limit of this data set helps to constrain future observations. In order to determine a period for Eris, new data would have to be more sensitive than these magnitude change detection limits. These results also make the 5-day period proposed by Carraro et al. (2006) unlikely, as this data set shows no periodogram peaks at that frequency.

Thesis Supervisor: Professor Richard P. Binzel
Massachusetts Institute of Technology

Introduction

Eris or 2003UB313

Eris was discovered on January 5, 2005 by the Caltech team of Brown, Trujillo, and Rabinowitz (Brown, et al. 2005). It was discovered as part of a Kuiper Belt Object survey that was being conducted at Palomar Observatory, the same project that discovered the KBO Sedna. Eris was the 4th brightest object in the Kuiper Belt, which is very impressive because it is much farther away than Pluto, 2003 FY9, and 2003 EL61. It has a V magnitude of 18.8 (Brown, et al. 2006). The orbit of Eris was traced backward, and the dwarf planet was identified in a plate taken in 1989 at the UK Schmidt Telescope (Brown, et al. 2005). Using this 16-year data point spread allowed for calculation of the orbit quite precisely.

Once Brown et al. had calculated the Dwarf Planet's orbit, it was clear that Eris' orbital characteristics mark it as a typical member of the scattered Kuiper Belt (2005). It has a semimajor axis of 67.89 ± 0.01 AU, an eccentricity of 0.4378 ± 0.0001 , and an inclination of 43.993 ± 0.001 degrees. The object appears so faint because Eris is currently at 97 AU, very close to aphelion. As it progresses along its 557-year orbit, Eris will eventually reach perihelion at 38.2 AU. Eris' known properties are displayed in Table 1.

Properties of Eris

Semimajor Axis	67.89 ± 0.01 AU
Eccentricity	0.4378 ± 0.0001
Inclination	43.993 ± 0.001 degrees
Orbital Period	203,500 days
Radius	2400 ± 100 km
Albedo	0.86 ± 0.07

Table 1. Properties of Eris. This table displays the known properties of the Dwarf Planet Eris, taken from Brown et al. 2006.

When Eris was discovered, it was estimated to be reasonably larger than Pluto, because it was expected to have an average albedo. More recent work with the Hubble telescope, however, allowed direct measurement of the size of Eris. Surprisingly, Eris was discovered to have an albedo of $86\% \pm 7\%$ (Brown, et al. 2006 Mar.). This was a much higher albedo than expected, and adding this factor to the calculations dropped the estimated size of the dwarf planet to a radius only about 5% larger than Pluto. The diameter of Eris was found to be 34.3 ± 1.4 mas, or 2400 ± 100 km. This very high albedo, however, is scientifically fascinating.

The surface of Eris is much less red than Pluto, appearing to be neutral in color, but has similar methane absorption lines (Brown, et al. 2005). The redness of Pluto's surface is interpreted to be irradiated complex organics. If the same process occurs on Eris, there would have to be a countering process, such as methane resurfacing, to create this brighter surface. Current spectroscopic measurements suggest that on Eris the methane is primarily pure and frozen on the surface. This high eccentricity of the Dwarf Planet dictates that Eris will have significant seasonal changes because of the variation in distances to the sun. At perihelion, Eris is projected to look much like Pluto, with dark

distances to the sun. At perihelion, Eris is projected to look much like Pluto, with dark red patches and lighter areas. Brown et al. speculates that the surface of Eris is currently so bright because as the dwarf planet moves farther from the sun, the methane freezes out and resurfaces it (2005). This homogenization of the surface is very important for this project because it predicts very little brightness variation in the object. This property makes detecting a period through changes in flux very difficult.

Recent images of Eris have discovered that it has a small satellite. Eris was imaged using the Keck LGS AO system in the K' filter. A satellite was discovered with an estimated orbital period of 14 days. Named Dysnomia, the moon is quite small, less than 200 km across (Brown, et al 2006 Feb). It is only about 2% of the brightness of Eris. Dysnomia can be seen to the right of Eris in Figure 1. Fortunately, this satellite is not large enough to impact the flux calculations for Eris.

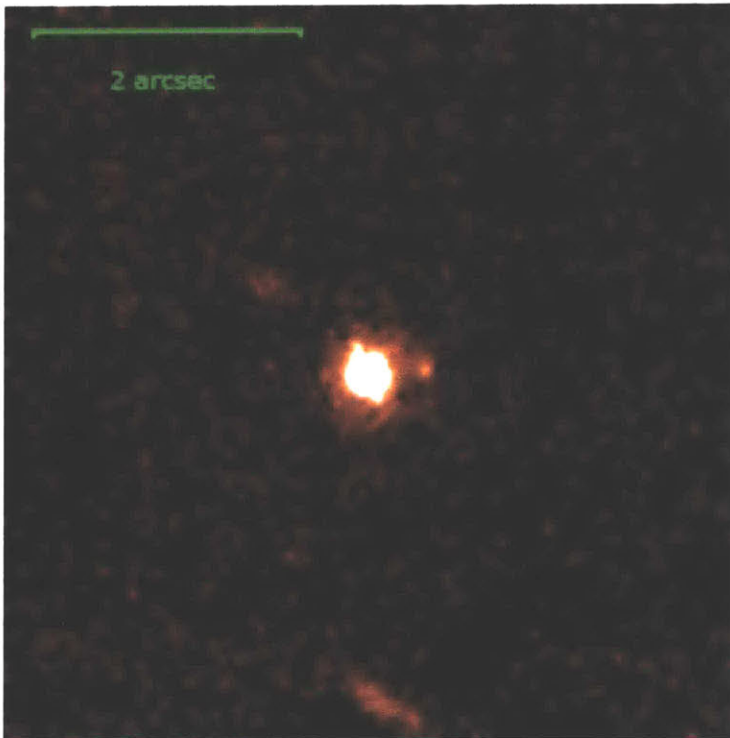


Figure 1. Eris and its Moon Dysnomia. This image shows Eris with its 200 km moon Dysnomia on the right. This picture of Eris was taken as part of a KBO satellite survey by Brown et al. in 2006.

Time Series Photometry

Photometric observations have been used to constrain the rotation rates of other Kuiper Belt Objects and some comets. For this process, a series of observations is taken over a long period of time. The more full rotations of the object that are viewed, the more likely it is that a period will be detected. An example of this process can be found in an analysis of 2003 EL61 data by Rabinowitz et al. (2006).

A time series photometry method was applied to 2003 EL61, a KBO discovered in December of 2004 (Rabinowitz et al. 2006). This object is closer and brighter than Eris, at 51 AU and a magnitude of 17.5. The data for this project were taken on the Small and Moderate Aperture Research Telescope System (SMARTS) 1.3 meter telescope. The images were taken in B, V, R, and I filters. To avoid finding only a 24-hour period due to the rotation of the fixed telescope on the earth, additional observations were taken at Palomar Observatory and Tenagra Observatory. The image reduction included nightly bias frames, and twilight flats. Absolute magnitudes were calculated using Landolt standard stars. The magnitudes of these stars in each frame were used to calculate the aperture size used in the flux calculations. The mean magnitude of EL61 and the standard stars were used to correlate the observations at the different sites. (A more detailed discussion is found in Rabinowitz et al. 2006).

Once the data on EL61 were obtained, it was obvious that the scatter in the observations was larger than the error in each observation. A periodogram was applied to the data, and the best-fit periods were determined. These two periods were 0.08 days and 0.16 days. The only other periods that appeared in the data were integer multiples of these periods. For both of these periods, the relative brightness of EL61 was plotted

against the rotational phase. The better-fit period was judged to be the double peaked light curve. This period was chosen because it has a better chi-squared fit and is more dynamically likely. The data is shown plotted over this period below, in Figure 2. This figure was taken directly from Rabinowitz et al. 2006. Their analysis of EL61 is an example of successful differential photometry and the discovery of a period using a periodogram.

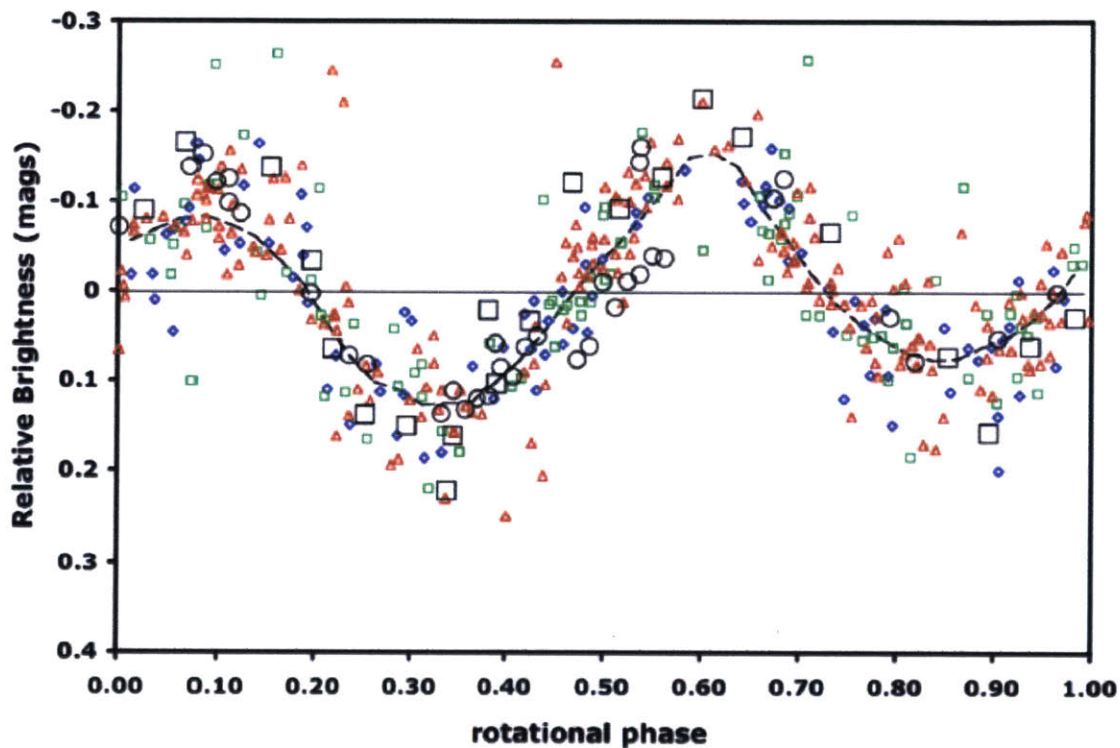


Figure 2. EL61 Data from Rabinowitz et al. 2006. This is Figure 3 from Rabinowitz et al. 2006. It displays the EL61 data plotted over the most likely period, 3.194 hours. The fit was better with a double peaked light curve, and it is visually evident that the two peaks and valleys have different amplitudes. The different colored points represent different filters, and the dashed line is a result of binning the data points in 40 different bins. Amore detailed explanation can be found in Rabinowitz et al. 2006.

Another example of time series photometry being used to determine the period of KBOs can be found in Lacerda and Luu, 2005. This paper looked at the magnitude changes of 10 different Kuiper Belt Objects for periodicity. They found 3 of the 10 to have amplitudes larger than 0.15 magnitudes, which is comparable to the detection limit

of this set of Eris data. The data for the 10 KBOs were taken at the Isaac Newton and William Herschel telescopes and were reduced using standard procedures. An aperture photometry procedure was used to generate the magnitudes and errors, which were standardized using a large number of stars in all frames. Landolt standard stars were used to calibrate the absolute magnitude of the objects of interest.

Lacerda and Luu generated light curves for their objects. To determine if the variance of the object was significant (detectable above their errors), histograms of comparison stars and the object were plotted. The reference stars should vary the least, followed by the comparison stars. The object should be isolated at a higher variation. This indicates that its changes in brightness are significant. If the KBO is included in the cluster of reference stars, it is unlikely that the variations are detectable. This same information is also plotted as magnitude versus variance, where KBOs with a significant signal can be seen well above the plotted arc of stars. To test for a period, Lacerda and Luu used a phase dispersion minimization method, testing periods from 2 to 24 hours. They also ran a verification method where they randomized the magnitudes within their error bars and used the PDM again. The amplitudes for the periods were also determined. A more detailed discussion can be found in Lacerda and Luu 2005.

Time series photometry has been used successfully by many other groups of astronomers for Kuiper Belt Objects, asteroids, and even comets. This technique is very powerful because it detects the period of an object's rotation and the amplitude of its brightness variation. These values can be used to constrain the shape, structure, and formation history of an object.

Anticipated Results

The magnitude variation of Kuiper Belt Objects is believed to be caused by aspherical shape, surface features, or changes in surface albedo (Lacerda and Luu, 2005). As objects rotate, the cross-section of the object that is visible from Earth changes, resulting in flux variations. This brightness variation is periodic. The goal of time series photometry is to measure this variation and calculate the period of the object.

When a period is determined, the speed at which the object is rotating can constrain its structure and shape (Lacerda and Luu, 2005). The strength of the rock dictates the breakup velocity of the object. If an object is discovered to be rotating very quickly, it means that the rocks must have some strength, instead of the 'rubble pile' structure.

Light curves that appear 'flat' can be a result of several different factors. The object may simply have a very low variation in brightness. This would imply either a spherical body or a body of any shape with its spin axis lined up with the observation point. Either of these geometries would result in a constant surface area. This 'flat' light curve does prove that any variations of the body's brightness are below the detection level of the data, and can be used to set an upper limit in brightness variation. These results are useful in planning future observations.

The amplitude of the magnitude variation gives information about the body. A very high amplitude is usually indicative of an aspherical shape. Large amplitudes result because a larger side reflects a lot of light, but the smaller face reflects much less light. These changes in surface area produce large magnitude variations viewed from Earth. Smaller amplitude variations still give a good deal of information. On Pluto, the flux

variations have been used to map out the areas of higher and lower albedo on the surface of the dwarf planet. It would be very useful to have similar information about the Dwarf Planet Eris.

Previous Time Series Photometry of Eris

Time series photometry of Eris was attempted by Carraro, Maris, Bertin, and Parisi in 2006. Their data were taken over 5 consecutive nights with the Y4KCam CCD on the Yale 1.0 meter telescope at the Cerro Tololo Interamerican Observatory (Carraro, et al. 2006). Images were taken in B, V, R, and I filters for 300-600 second exposures. The images were reduced, and an aperture photometry routine in IRAF was used to calculate magnitudes. Five stars in all images were used as a standard for the Eris magnitudes.

Several periods were tested by a chi-squared fit. Many were rejected due to aliasing with Earth's orbit. Their data show a higher variance than they believe could be due to their random errors or calibration errors (Carraro et al. 2006). They conclude that the period of Eris is probably 5 days or more, with an amplitude of 0.05 magnitudes (full amplitude ~ 0.1 magnitudes).

Because Carraro et al. had so few data points, they had some difficulty producing a convincing period. It also appears that they underestimated some of their error bars, and did not actually have the accuracy they report. This would imply that their detection of brightness variations is within their error, and not truly changes in Eris' brightness.

These new observations of Eris, however, should be more robust. They are not limited by Earth's rotation rate, because the images are taken by a spacecraft. The errors in the images are better understood, as there are no atmospheric fluctuations to worry about. The new Eris images were tested for periods between 4 and 120 hours to include this possible 5-day period, without similar results.

Data Collection

Data were collected using the satellite Swift. Swift was designed to detect and image Gamma Ray Bursts. It therefore has a fast slew rate and can perform other observations while waiting for Gamma Ray Burst events. Swift is equipped with a 30 cm Ritchey-Chretien reflector, the Ultraviolet/Optical Telescope (UVOT) (Saurabh et al. 2006). This telescope uses microchannel-intensified CCD detectors, which maximize signal to noise (Li et al. 2005). It also has a Burst Alert Telescope and the X-Ray Telescope. The Swift UVOT can take images in the U, B, and V bands. This combination of telescopes allows Swift to image gamma ray bursts and their afterglow in the gamma-ray, X-ray, and ultraviolet/optical wavelengths. Swift images require a good deal of processing, much of which is done before the images are even made ready for the astronomers. The images are rotated and calibrated. Exposure maps are also provided to assist with reduction. The magnitude zero points and magnitude with count-rate of 1 are intensively calculated scales to convert from instrument magnitude to absolute magnitude (Li et al. 2005).

For this project, the data were taken using the UVOT in the B filter over 23 nights. Eris is marked in Figure 3, to give some idea of its relative brightness. There are 288 total images, of which 266 were used in the analysis. Some images were eliminated because the object was too close to the edge of the frame. Images were also rejected when the signal to noise was too high, due to either a shorter exposure time or instrument problems. Comparison images can be seen in Figure 4. The remaining good images were analyzed for the flux of Eris and 33 other stars in the frame.

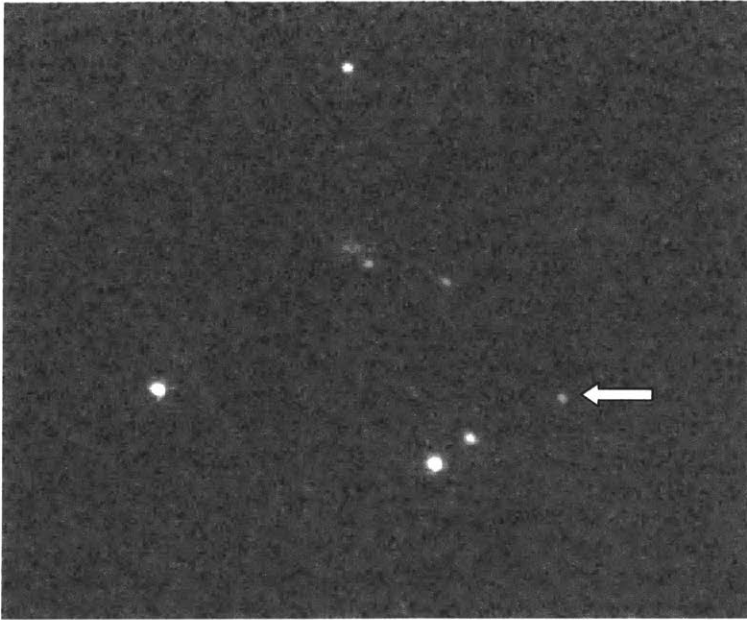


Figure 3. Swift Image of Eris. This is an image of Eris taken by the satellite Swift. Eris is indicated by the white arrow.

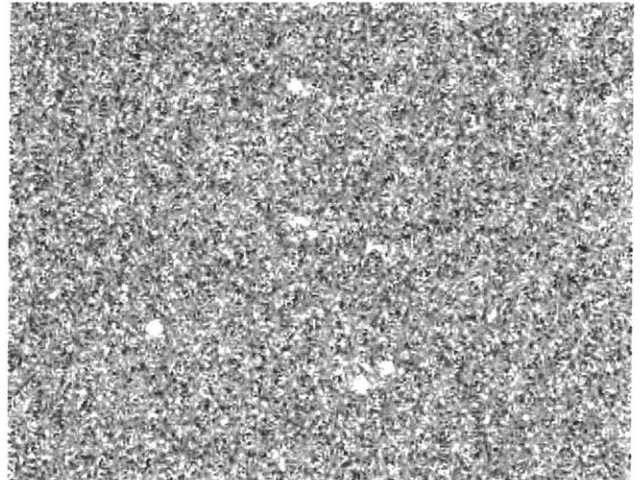
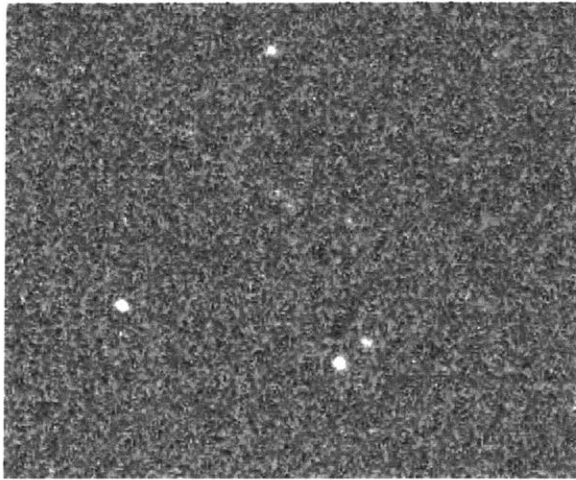


Figure 4. Image Comparison. These images show that not all of the image quality is a result of exposure time. The left image (41) was exposed for 77 seconds, and the right image (62) was exposed for 121 seconds.

Methods

The first step in calculating the flux was to locate Eris and a reference star in all of the images. The offset in pixels of 32 other reference stars was recorded, and positions of the stars were calculated in all frames. The coordinates of the object and selected stars were written into an excel file along with the image titles, indexes, and other relevant information. This file was read into IDL as a structure array. The array was designed to accept the calculated values for the flux of Eris and selected stars.

The flux of Eris and the selected stars was calculated using the “aper” procedure in IDL. This procedure invokes aperture photometry to find the flux and error of an object. After testing a range of aperture values, an aperture radius of 2.5 pixels was selected for the 2x2 binned images and 5.0 pixels for the 1x1 binned images. The aperture of the comparison stars was increased to 5.0 and 10.0 pixels to account for the fact that many of the reference stars were brighter than Eris. The routine also calculated sky values, using an inner and outer sky apertures of 10 and 30 pixels.

As mentioned previously, the Swift UVOT provided an exposure map for each image. By dividing the regular images by the exposure maps and running the “aper” procedure a second time, the number of photons per second was calculated. This was a crucial step because many of the images had different exposure times. The midpoint of the exposure time was also calculated to facilitate accurate comparison. The flux, in photons per second, was converted to magnitude using the equations and conversion factors provided in Li et al. 2005. For the B filter used in these images, the photometric

zero point $ZP = 18.92 \pm 0.01$ mag, and the magnitude where the true count rate is 1, $m_{\infty} = 14.16 \pm 0.02$ mag.

$$m_{\text{UVOT}} = -2.5 \log_{10}(\text{counts/sec}) + ZP \quad \text{Equation 1}$$

$$\mu = -\ln[1 - 10^{-0.4(m_{\text{UVOT}} - m_{\infty})}] \quad \text{Equation 2}$$

$$m_{\text{Landolt}} = -2.5 \log_{10}(\mu) + m_{\infty} \quad \text{Equation 3}$$

(Li et al. 2005)

These formulas allow for the calculation of magnitude. For this data set, the average magnitude of Eris was found to be 19.435. Once the magnitudes were calculated for each image, the good data points were plotted as magnitude verses midpoint time in Figure 5.

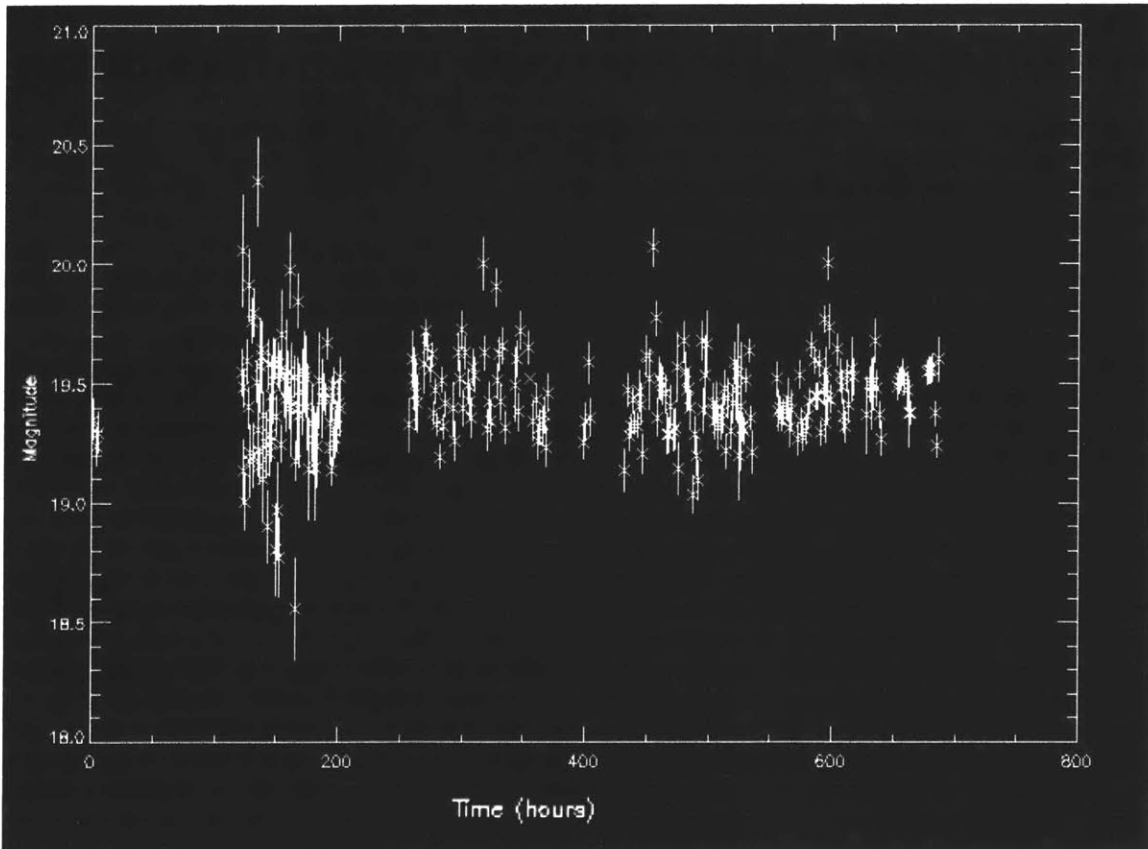


Figure 5. Eris Magnitudes. This plot shows the Eris magnitudes in each frame verses the midpoint time of the image without a standard star correction.

The next step in the data reduction was to take into account the brightness of the reference stars in the frames. As with Eris, the flux per second of each star was converted to magnitude. Because of the motion of Eris and the desirability of avoiding nearby bright stars, many of the comparison stars do not appear in every frame. This meant the data required an ensemble photometry method. Ensemble photometry is a very powerful method, using a least squares fit to calculate the correction applied to each image. Using numerous stars increases the statistical accuracy of the photometry and averages out residual systematic flat-field errors for comparison stars (Honeycutt 1992). The stars are all weighted, and in any frame that the star does not appear, its weight is set to zero. Because of this, stars that appear in many but not all of the frames can be used to calibrate the images.

The magnitudes of the reference stars were analyzed by an IDL routine ‘ensemble_phot.’ This routine takes input arrays of star magnitudes and magnitude error and returns an array containing the magnitude correction for each image. The user can also specify exclusion criteria. Exclusions can be a specific star in a specific image, all stars in a specific image, or specific stars in all images. In these data, one bad image was masked as well as 6 of the 33 stars that were possibly periodic. The star-image combinations that fell outside the frame were also excluded from the fit. The magnitude correction was subtracted from the Eris magnitude in each image, and the results were plotted in Figure 6.

If there is a detectable variation in Eris’ brightness that is related to its rotation, these data could be modeled with a periodic solution. To check for periodicity of the data set, an IDL function called “periods” was used. This procedure iterated through periods

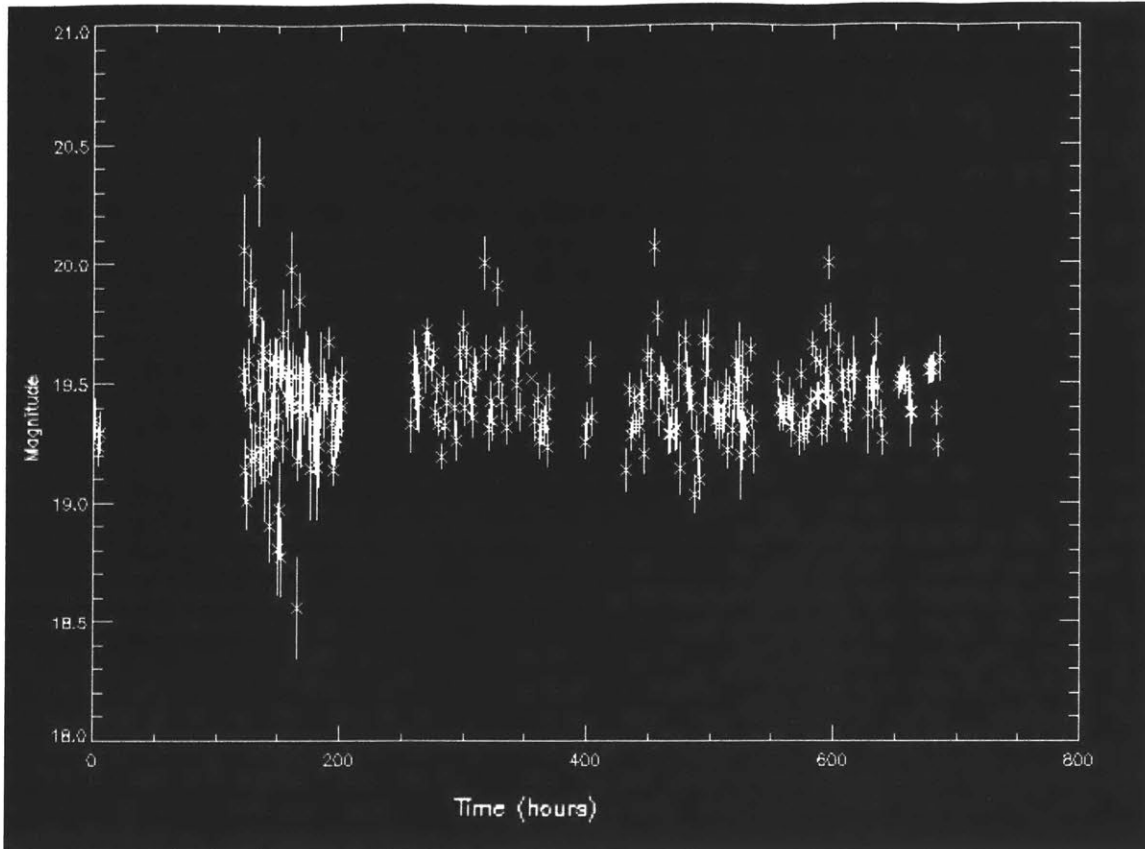


Figure 6. Corrected Eris Magnitudes. This plot shows the corrected magnitude of Eris versus midpoint time. The images have been corrected using 33 standard stars in the frames.

from 4 hours to 120 hours in 6000 steps of about $4.02e-5$ hours each. For each periodic solution, the program calculates the strength of the detection. The highest peaks in the graph represent the possible solutions. Generally, a peak with a value of 12 or more is an almost indisputable solution. Values of 7 or 8 and above are good possible solutions, which want some more verification. The periodogram solution for the Eris data (shown in Figure 7) is not very significant. This means that the data were probably not good enough for the changes in magnitude of Eris to be detected.

To better understand the significance levels of the peaks, the data set was randomized by reassigning the magnitude and time values. Then a periodogram was calculated for each of these randomizations, and the significance of the highest point was

recorded. This was done for 10,000 randomizations of the data set, which generated a list of significance values. These data sets were random, and thus should not really generate any periodic solutions. The variation in the significance was calculated to give an idea of what levels of false signals our data points could generate. One sigma above false positives was 6.682, two sigma was 8.811, and a three sigma significance was 11.728. This result is very telling, as the periodogram for our data gives a peak at 13.99 hours with a significance of just under 1 sigma, 6.244. This means that our data are not giving a detectable signal.

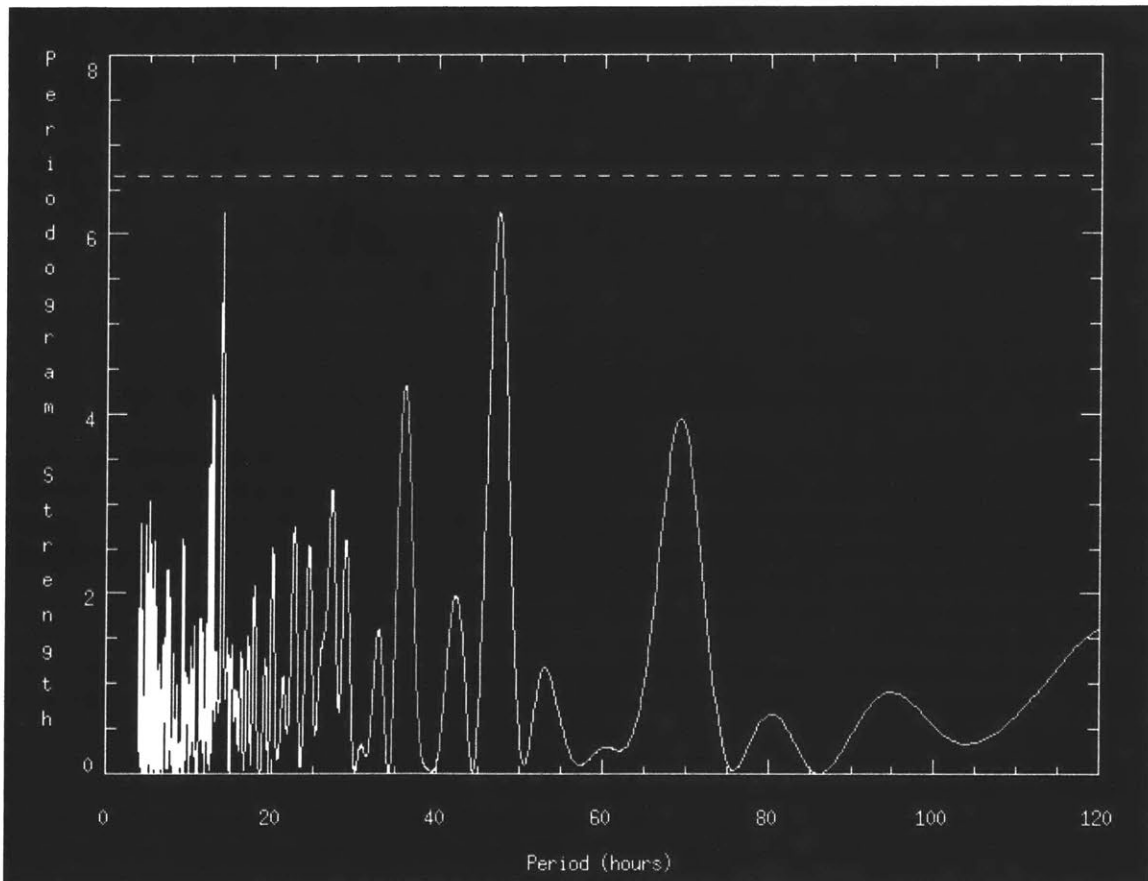


Figure 7. Periodogram Results. This is the result of running a periodogram (period search procedure) on the corrected Eris data. The highest peak is at 13.99 hours, but is not very significant. It is below a 1 sigma level detection, shown as the dashed line in this plot.

Next, the data were viewed in a wrapped plot. Here, the data set is plotted based on where it falls in the unlikely 14-hour period. What is pictured here is a plot of all of the data superimposed over one period. This is visible in Figure 8, where the overall mean magnitude is a dotted line, and a solid line shows the local mean value. When the wrapped data are examined over the period with the highest significance, the results unfortunately do not appear any more conclusive.

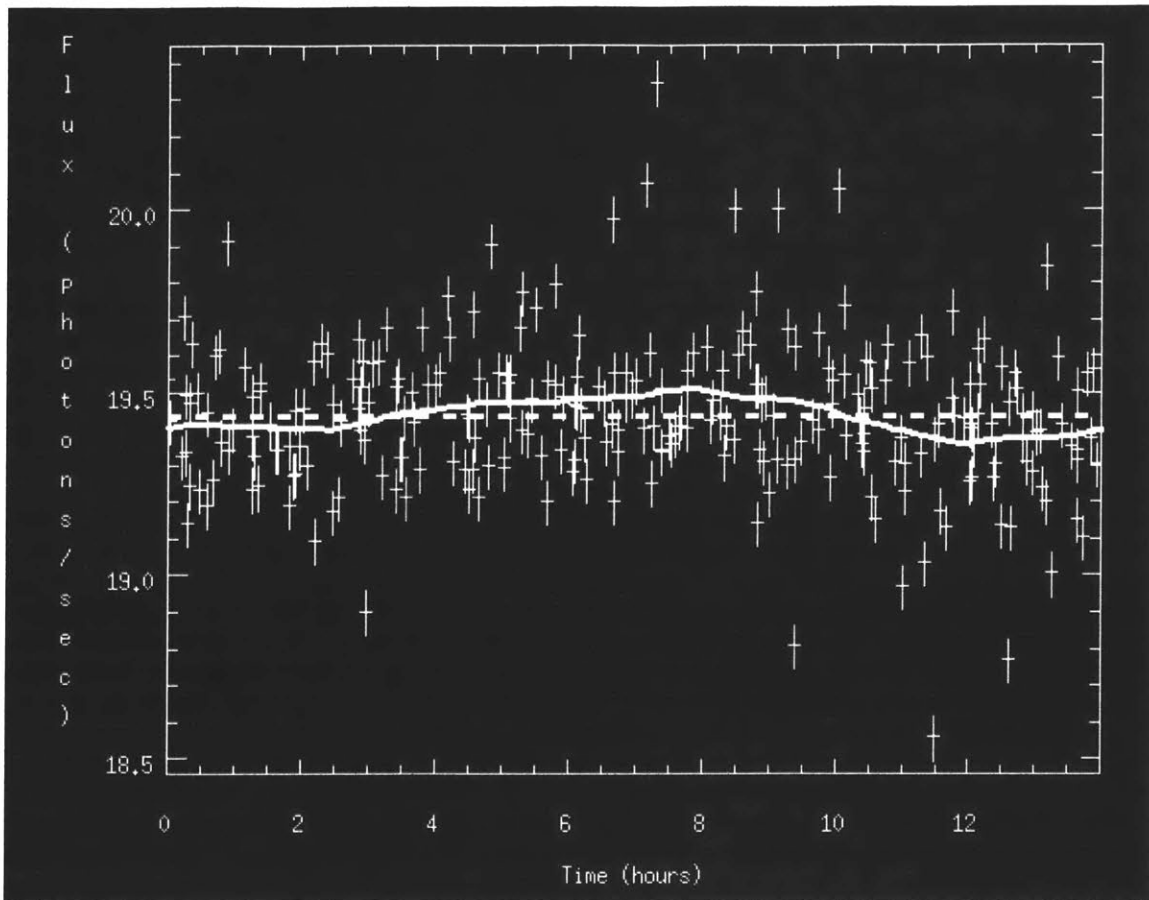


Figure 8. Wrapped Plot of Eris Data. Here, the data on Eris brightness are plotted over one rotation for the most likely period of 14 hours. The dashed line shows the mean magnitude of Eris, and the solid line shows the local mean magnitude. This image does not give a convincing argument for the likelihood of the signal.

To determine if the data should be showing a signal, the standard deviation of the flux of Eris was compared to the standard deviation of the flux of the comparison stars.

This is shown in Figure 9. In this plot it is clear that the flux variations of Eris are on the

same scale as the flux variations of the stars. This makes it unlikely that there is a detectable period in these data.

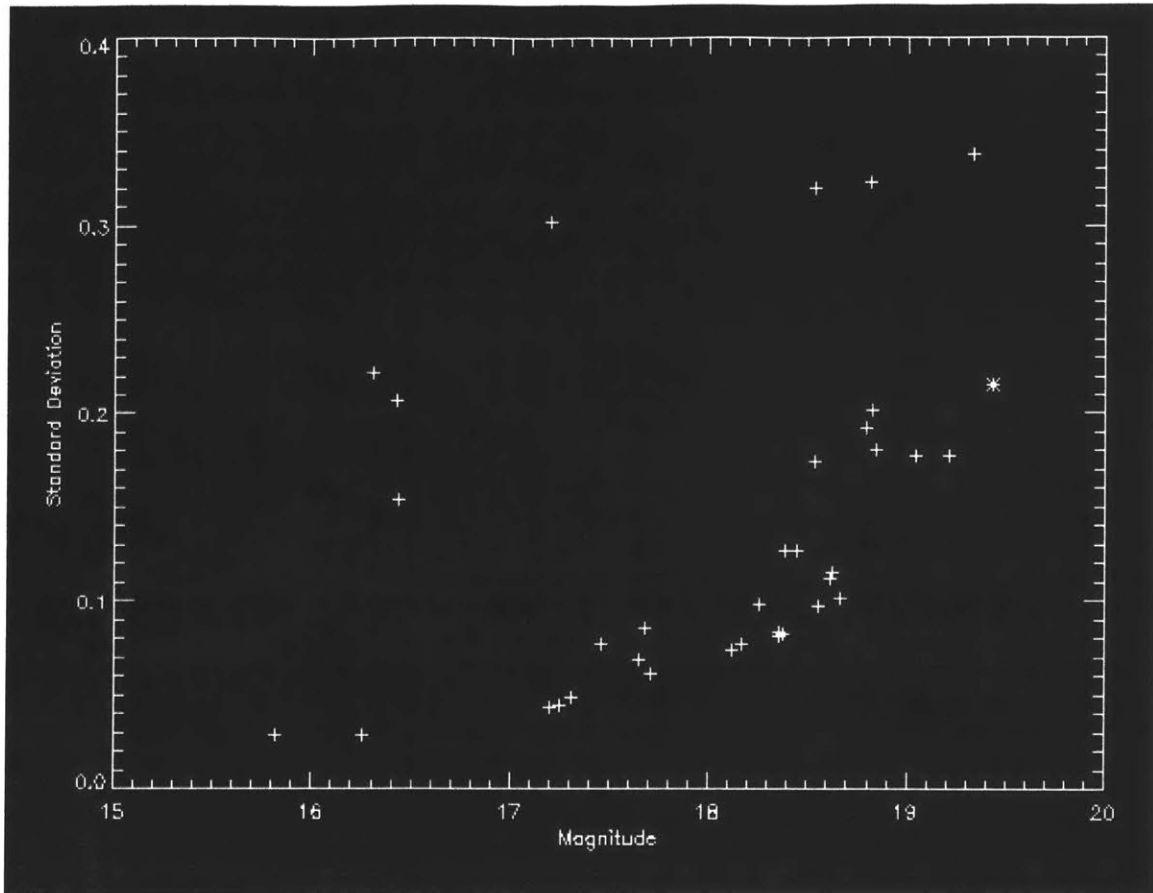


Figure 9. Magnitude Standard Deviations. This is a plot of the 33 standard stars (indicated by the + signs) and Eris (indicated by the * symbol). The objects are plotted by magnitude versus standard deviation of the magnitude. Most of the stars fall on an upward arch, indicating the accuracy of the data. Eris falls within this arch, so it is unlikely that the variations in Eris' flux are significant.

The data analyzed here did not reveal a period for Eris. It is important, therefore, to examine the data and determine what signal strength would have been detected. These data will give an upper limit on the flux variation of Eris. Knowing the minimum detectable variation will help to guide future observations. This limit will be especially useful in ruling out observation options that are less sensitive than the one used to generate these data.

To determine the sensitivity of these data, a false sinusoidal signal was inserted into these data. A sine function was defined, and at each time t where there was a measurement of Eris flux, the signals were added together. The full amplitude of the false signal is A , and the period of the false signal is represented by P .

$$m_{\text{False}} = (A/2)\sin(2\pi(t)/P) \quad \text{Equation 4}$$

$$m_{\text{Total}} = m_{\text{False}} + m_{\text{Eris}} \quad \text{Equation 5}$$

The full amplitude A and period P were varied to determine whether or not the signal could be detected in m_{Total} . For each period, amplitudes were tested until one was found to be of two-sigma significance. (These data were reshuffled for each new value to find the significance.) The results are recorded in Table 2. For comparison, Figure 10 shows the periodograms and wrapped plots for just the Eris magnitude and the cases listed in the table.

Detectable Signals

Period of False Signal (hours)	Amplitude with 2 Sigma Significance
6	0.160
12	0.125
18	0.155
24	0.185

Table 2. Detectable Signals. This table shows the amplitudes of the false signals that were required to produce a periodogram peak with 2 sigma significance. This table shows the detection level of the data.

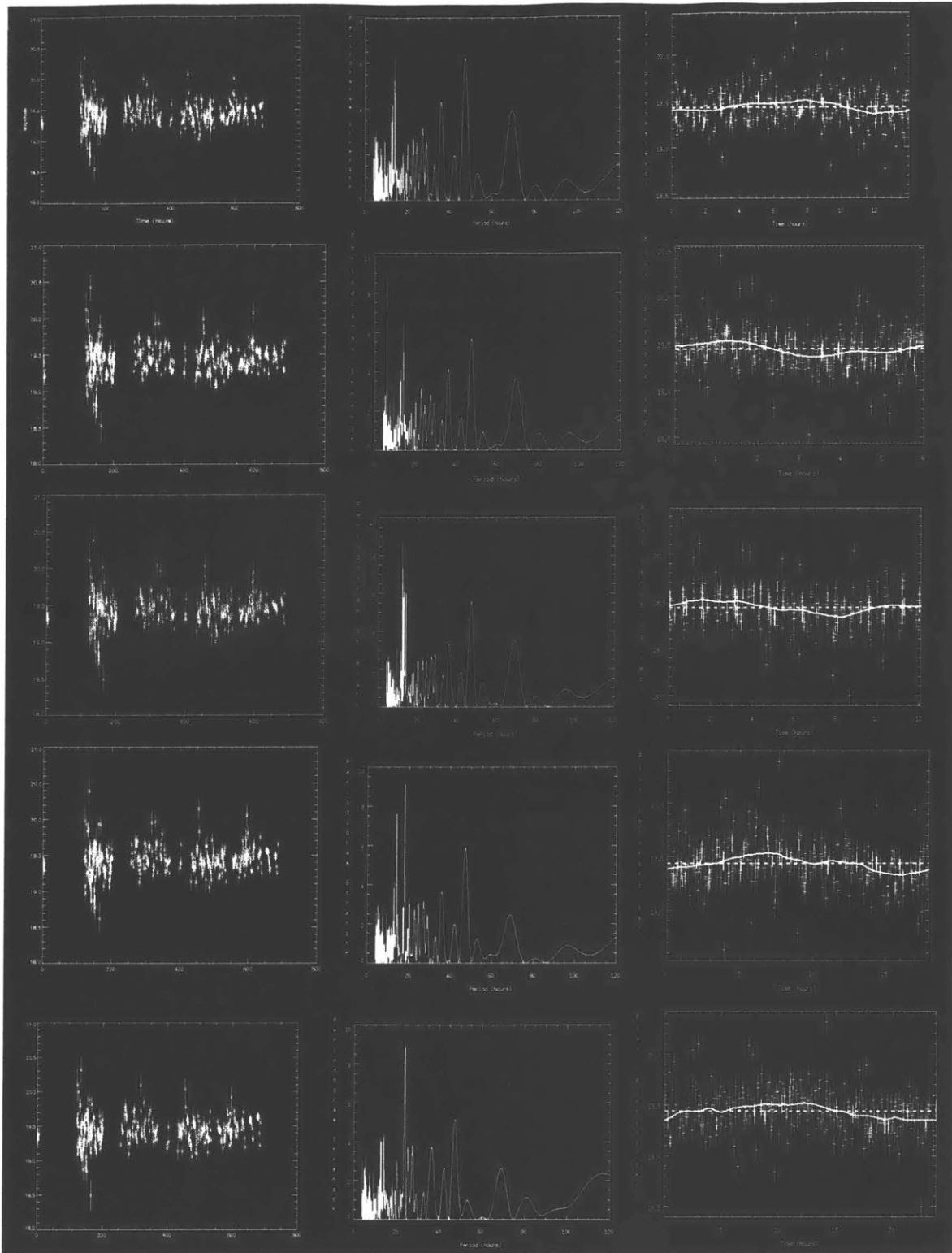


Figure 10. Comparison Data Plots. Here all of the plots are displayed: the magnitude versus time, periodogram, and wrapped plots (left to right). From top to bottom, there is Eris Data, Eris Data plus a 6 hour period, 12 hour period, 18 hour period, and a 24 hour period.

Analysis

It is unfortunate that these data did not convincingly determine the rotational period of Eris. The signal to noise was simply not high enough for the periodogram to detect a signal. The large amount of data points due to the extent of our survey should have allowed us to detect even small periodic amplitude changes. It is not surprising that Eris has a small amplitude of magnitude variations. Eris has a very high albedo, which is suspected to be a result of frequent resurfacing of methane ice. This would imply very small albedo variations across the surface. The “dwarf planet” by definition is also large enough to be spherical in shape, which eliminates shape as a contributor to brightness variations. This low amplitude of magnitude change still provides useful information.

These data also spanned a long period of time, which facilitates the detection of longer periods. This was very useful because of the possible detection of a 5-day period by Carraro et al. in 2006. The amplitude of their signal was over 0.1 magnitudes, and should have been detectable in this data set. (It would have been a weak detection in these data, but should have been visible on the periodogram.) The periodogram developed from these data does not show any possible signals around 5 days. This makes it unlikely that Eris has a 5-day period. The period of Eris is, therefore, completely unresolved.

These data do provide some valuable conclusions about the maximum amplitude of Eris' magnitude variations. The low variability supports the information currently known about the dwarf planet's shape and surface processes. It also helps to constrain future observations. Any future attempts to find the period of Eris will need to be able to

resolve magnitude variations of less than 0.15, preferably less than 0.10. Anything greater than that will demonstrate the same nondetection illustrated in this data set. The values shown in Table 2 can be used to determine the required signal to noise to either lower the maximum possible amplitude of Eris or detect a period. Given the incredibly high albedo of Eris, it is very possible that variations are on an incredibly small scale. Knowing the minimum required accuracy for Eris flux calculations will help astronomers to choose observing sites and instruments.

Conclusions

The goal of this project was to determine the orbital period of the dwarf planet Eris. Unfortunately, the resolution of the data set was not good enough to facilitate the detection of a period. This is not entirely surprising given what is currently known about Eris. The dwarf planet has an incredibly high albedo of about 86%, which implies frequent resurfacing of the surface ices. This makes it unlikely that there are large albedo variations across the surface of Eris. Eris is also larger than Pluto, and should be quite spherical. This also makes it unlikely that Eris would have high albedo variations due to shape or surface features.

Instead of the rotation period, the ultimate results from these data are the minimum signals that could have been detected in the data. These results are given in the form of the minimum full amplitude of the variation in Eris' magnitude that could have been indisputably detected. These amplitudes are the values at which the significance of the period detected is two sigma. The actual changes in Eris' magnitude due to its rotation have to be smaller than the recorded amplitudes, or they would have been detected in this data.

These results are actually quite useful in the planning of new observations. They give a limit on the telescope power and signal to noise required to make further observations useful. Any new project should attempt to be able to resolve magnitude changes less than 0.1, or there is little chance of detecting a period in Eris' magnitude.

Works Cited

- M. E. Brown, M. A. van Dam, A. H. Bouchez, D. Le Mignant, R. D. Campbell, J. C. Y. Chin, A. Conrad, S. K. Hartman, E. M. Johansson, R. E. Lafon, D. L. Rabinowitz, P. J. Stomski, Jr., D. M. Summers, C. A. Trujillo, and P. L. Wizinowich. “Satellites of the Largest Kuiper Belt Objects.” *The Astrophysical Journal*, 639:L43–L46, 2006 March 1, *published 2006 February 10*.
- M. E. Brown, E. L. Schaller, H. G. Roe, D. L. Rabinowitz, and C. A. Trujillo. “Direct Measurement of the Size of 2003 UB313 from the *Hubble Space Telescope*.” *The Astrophysical Journal*, 643: L61–L63, 2006 May 20, *published 2006 May 4*.
- M. E. Brown, C. A. Trujillo, and D. L. Rabinowitz. “Discovery of a Planetary-Sized Object in the Scattered Kuiper Belt.” *The Astrophysical Journal*, 635:L97–L100, 2005 December 10, *published 2005 November 22*.
- Carraro G., Maris, M., Bertin, D. and Parisi, M. G. “Time series photometry of the dwarf planet Eris (2003UB313).” *Astronomy & Astrophysics*, 460, L39-L42, 2006.
- Lacerda, Pedro. Luu, Jane. “Analysis of the Rotational Properties of Kuiper Belt Objects.” *The Astronomical Journal*, 131:2314–2326, 2006 April.
- Li, W., Jha, S., Filippenko, A., Bloom, J., Pooley, D., Foley, R., and Perley, D. “The Calibration of the *Swift* UVOT Optical Observations: A Recipe for Photometry.” *The Astronomical Society of the Pacific*, 118:37-61, 2006 January.
- Rabinowitz, David, Barkume, Kristina, Brown, Michael, Roe, Henry, Schwartz, Michael, Tourtellotte, Suzanne, and Trujillo, Chad. “Photometric Observations Constraining the size, shape, and albedo of 2003 EL61, a Rapidly rotating, Pluto-Sized Object in the Kuiper Belt.” *The Astrophysical Journal*, 639:1238–1251, 2006 March 10.
- Sheppard, Scott S, Jewitt, David C. “Time-Resolved Photometry of Kuiper Belt Objects: Rotations, Shapes and Phase Functions.” *The Astronomical Journal*, 124:1757–1775, 2002 September.